J. Plasma Physics (2013), *vol.* 79, *part* 2, *pp.* 153–161. © Cambridge University Press 2012
doi:10.1017/S0022377812000815

Electron heating in a multi-dipole plasma by electrostatic plugging

M. K. MISHRA[*,1] and A. PHUKAN[*,2]

[*]Centre of Plasma Physics, Institute for Plasma Research, Tepesia, Sonapur, Assam-782402, India
[1]Department of Physics, Baosi Banikanta Kakati College, Nagaon, Barpeta, Assam-781311, India
(mishra.mrinal@rediffmail.com)
[2]Department of Physics, Madhabdev College, Narayanpur, Lakhimpur, Assam-784164, India

(Received 30 May 2012; revised 21 July 2012; accepted 26 July 2012; first published online 12 September 2012)

Abstract. The effect of the electrostatic confinement potential on electron number densities and electron temperatures under bi-Maxwellian approximation for electron distribution function has been studied in an electrostatically plugged multi-dipole argon plasma system. Electrostatic plugging is implemented by biasing the electrically isolated multi-dipole magnetic cage. Experimental results show that the density ratio (N) and temperature ratio (T) of the two electron groups can be controlled by changing the voltage applied to the magnetic cage. Out of the two groups of electrons, one group has the cold electrons, which are plasma electrons produced by the ionization process, and the other group has the hot primary electrons.

1. Introduction

Filament discharge plasmas produced inside a multi-dipole device have been widely used for studying basic phenomena in plasma (Leung et al. 1975). Inside the multi-dipole magnetic cage, the chief mechanism of plasma generation is the electron-neutral collisions that occur between the primary electrons emitted from the hot filaments and the background gas. The thermionically emitted primary electrons that are accelerated from the filaments by applying a discharge voltage (V_D) between filaments and the cage, ionize the neutral gas producing the plasma. The filaments act as a cathode and the magnetic cage acts as an anode. The increase in plasma density can be achieved by efficient confinement of primary ionizing electrons. To trap these ionizing electrons, the walls of the cage are lined with permanent magnets in rows of opposite polarity, which creates a magnetic barrier (Limpaecher and MacKenzie 1973). The generated magnetic field is very close to the walls and hence the main plasma region is field-free. However, Bosch and Merlino (1986) experimentally showed that confinement of both electrons and ions could be enhanced by the use of multi-dipole cage even if the plasma source is devoid of any primary electrons.

The plasma parameters in such a weakly ionized plasma are essential to study different particle elementary processes and plasma collective phenomena. Different techniques have been applied to control the plasma potentials and electron temperature in a multi-dipole device (Hershkowitz and Leung 1975; Hershkowitz et al. 1992; Phukan et al. 2007). It is widely recognized that plasma parameters are highly sensitive to the boundary conditions of the confining vessel. The role of magnetic filed and electrostatic field on plasma confinement has been studied for last few decades (Leung et al. 1976; Andreu et al. 1985).

In multi-dipole devices, if some external potential V_S is applied to the magnetic cage, then effective energy of the primary electrons will be $E_P \approx e\,(V_S \pm V_D)$, since the filament is biased at $-V_D$ with respect to the magnetic cage, and the primary electrons are accelerated by the plasma potential controlled externally by the applied bias voltage V_S (Hershkowitz et al. 1982; Cho et al. 1990). Thus, biasing the cage more positively increases the potential energy of the system, but it can also enhance electron loss.

In multi-dipole devices, it is generally accepted that at the lower limit of the gas pressure (less than about 10^{-4} mbar), there exists three groups of electrons (Ruscanu et al. 2000). These are (i) primary or ionizing electrons, (ii) secondary or hot electrons, and (iii) ultimate or cold electrons. The primary group is formed as a mono-energetic group due to the acceleration of filament electrons into cathodic sheath. In general, it is also accepted that ionization of the neutral gas atoms due to their collisions with primary electrons may produce the other two bi-Maxwellian groups of electrons. The secondary or hot electrons result as degrading process of the primaries. The ultimate or cold electrons are born in pair with ions as a result of ionization. But at relatively high neutral pressure of 10^{-4} mbar or above, even primary electrons may behave as Maxwellian electrons (Holmes 1982; Oertl and Skoelv 1984). At sufficiently high neutral pressure, primary electrons may become indistinguishable from plasma electrons (cold) due to inelastic collisions (Chan et al. 1982). The present experiment is carried out at a fixed pressure of 5×10^{-4} mbar, and we have considered a two-component electron

https://doi.org/10.1017/S0022377812000815 Published online by Cambridge University Press

distribution, which is Maxwellian for both thermal (cold) and primary (hot) electrons (Mishra et al. 2007).

In this experiment, the effect of magnetic cage biasing voltage on the density and temperature of both hot and cold electrons are studied.

The experimental results presented in this paper may be helpful for plasma applications such as thin film deposition, plasma etching, and negative ion production. All these applications require high density and very low electron temperature for fruitful outcomes. The observed variation in electron temperature and density of the two electron groups with change in cage biasing voltage may help to find out the optimum condition for the above-mentioned applications.

In this paper, the words energy and temperature imply the same meaning.

2. Experimental setup

The experiment is carried out in a cylindrical shape, stainless steel chamber having a length of 120 cm and a diameter of 30 cm. The chamber wall is electrically grounded. The magnetic cage is cylindrical in shape having a length of 35 cm and a diameter of 25 cm. The magnetic cage consists of cubical strontium ferrite magnets with a surface field of 1.2 kilo-gauss, embedded inside stainless steel channels, which are arranged in a cylindrical shape and placed inside the chamber. The magnetic cage is electrically insulated from the chamber wall and is biased externally with respect to ground by a DC power supply, V_S. The sketch of the experimental setup with discharge circuit is shown in Fig. 1(a). The schematic diagram of the surface magnetic field produced by multi-dipole magnets, and the location of filaments inside the cage are shown in Fig. 1(b).

To evacuate the chamber to a base pressure of 4×10^{-6} mbar, a diffusion pump backed by a rotary pump is used. Argon gas is fed into the chamber and the plasma is produced by electron bombardment at 5×10^{-4} mbar by applying DC voltage (V_D) between the hot filaments and the magnetic cage. In the setup, the filaments act as a cathode and the magnetic cage acts as an anode. The discharge voltage V_D is maintained at –50 V, and the discharge current is maintained at 60 mA. The potential applied to the cage can be varied by changing the DC voltage (V_S). A plain Langmuir probe of diameter 4 mm is placed at the center of the cage to measure plasma parameters. The plasma potential is obtained from the probe potential that corresponds to the peak of the first derivative of probe characteristics (Phukan et al. 2007).

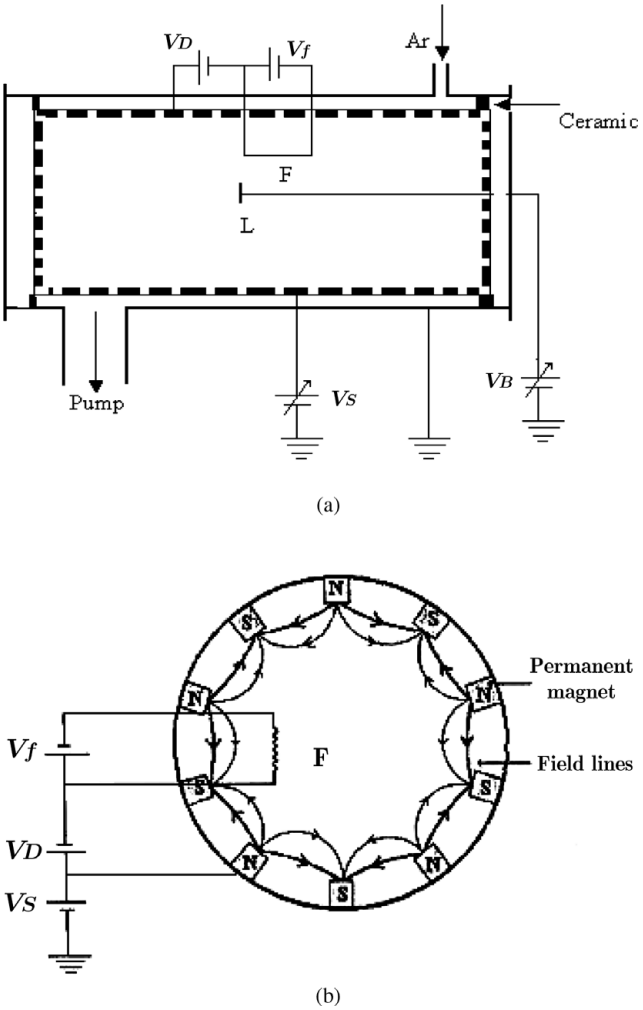


Figure 1. (a) Schematic diagram of the experimental setup. Here F is the filament and L is the plain Langmuir probe. V_f is the filament heating voltage, V_D is the discharge voltage, V_S is the cage biasing voltage, and V_B is the probe voltage. (b) The schematic diagram of the surface magnetic cusp field produced by the multi-dipole magnets and the location of the filaments inside the magnetic cage.

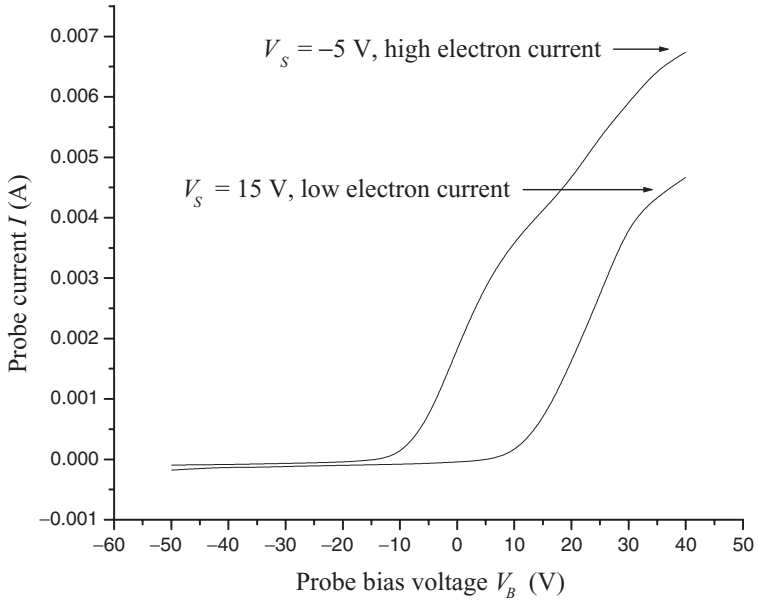
3. Results and discussion

3.1. Estimation of density and temperature of bi-Maxwellian electron plasma by Langmuir probe

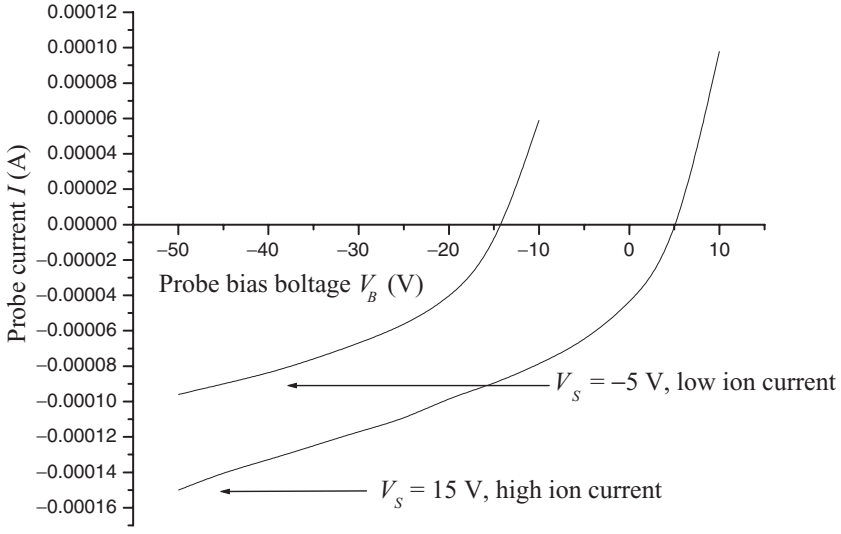
Plasma parameters, such as density and temperature, of both the electron groups along with ion density and plasma potential are measured at the center of the magnetic cage with the help of a plane Langmuir probe. The magnetic cage biasing voltage V_S is changed from –5 V to +15 V in steps of 5 V, while the discharge voltage and the discharge current are maintained at 50 V and 60 mA respectively.

In Fig. 2(a) and (b), Langmuir probe characteristics recorded at V_S = –5 V and +15 V are shown. It is observed that the electron saturation current decreases with an increase in ion current when the magnetic cage biasing voltage is changed from –5 V to +15 V. The plasma electrons (cold electrons) are lost to the cusp, which is further facilitated by the positive bias voltage. In other words, when the magnetic cage biasing voltage V_S is changed from negative to positive, the electrons experience an additional attractive force to move toward the cusp's wall, which enhances the loss of electrons at the cusp region of the magnetic cage. Therefore, a decrease in electron saturation current is observed. Since in steady state, the number of ions and

https://doi.org/10.1017/S0022377812000815 Published online by Cambridge University Press



(a)



(b)

Figure 2. (a) Langmuir probe characteristics recorded at $V_S = -5$ V and 15 V. The curve at $V_S = +15$ V shows reduced electron saturation current in comparison to the curve at $V_S = -5$ V. (b) The enlarged view of the probe characteristics showing ion saturation current recorded at $V_S = -5$ V and 15 V.

electrons created per second equals the ion and electron loss rates, the electron current leaving the plasma must be compensated by the ion current in bulk making the plasma more positive

In the probe characteristics, the electron distribution may be non-vanishing at least up to energies corresponding to the discharge voltage $-V_D$. The probe current (I_p) – voltage (V_B) characteristics are recorded below the discharge voltage $-V_D$ ($V_B < -V_D$) so that even primary electrons cannot contribute to the probe current, and the current collected by the probe is only due to ions.

Here, for each cage bias voltage V_S, we have recorded probe current up to probe bias of $V_B = -60$ V for the applied discharge voltage, $V_D = -50$ V, so that the probe current corresponding to $V_B = -60$ V is due to ions only. From this ion current (I_i), ion density (N_i) can be calculated from the Bohm ion current (Merlino 2007),

$$I_i = 0.6e\, N_i\, C_S A_P, \tag{1}$$

where e is the elementary charge, C_S is the ion acoustic speed, and A_P is the probe surface area.

Again, in order to obtain the actual electron current I_e, the ion current (I_i) is subtracted from the total probe current. The method of extrapolation of the ion current into the regime $V_B > -V_D$ may also apply for the proper determination of the actual electron current, I_e. This is shown in Fig. 3.

https://doi.org/10.1017/S0022377812000815 Published online by Cambridge University Press

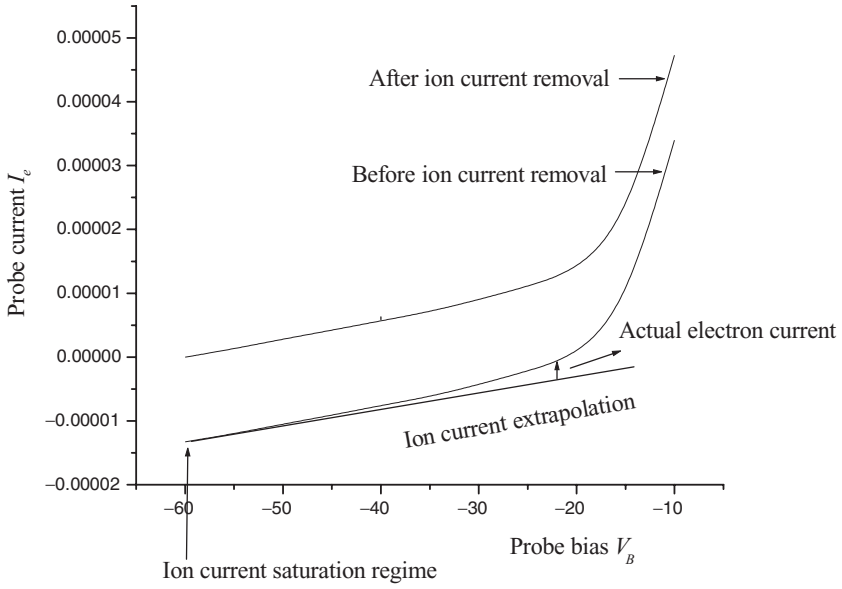


Figure 3. The ion current extrapolation is shown along with the actual electron current.

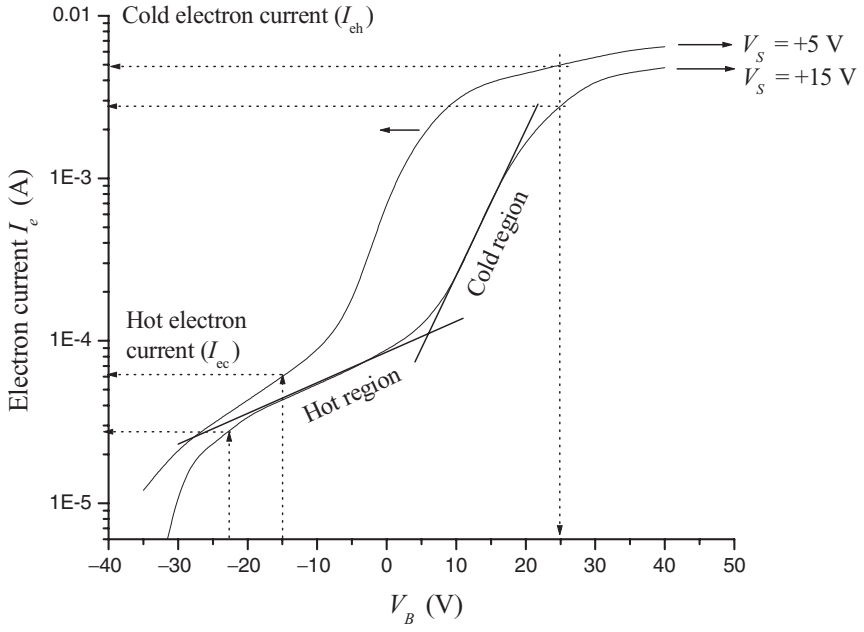


Figure 4. The semi-log plot of probe characteristics taken at $V_S = 5$ V and 15 V, showing the hot and cold electron temperature regions.

The electron current I_e is split up into a sum of bi-Maxwellian electron current (hot + cold) as observed from the semi-log plot in Fig. 4 for $V_S = 5$ V and 15 V. The $\ln(I_e)$ has pronounced a double-slope shape indicating a bi-Maxwellian EEDF (Pustylnik et al. 2006). The magnitude of current in the plot shows that the density of the hot electrons is much lower than that of the cold electrons (Pilling and Carnegie 2007). The temperature of each electron group is obtained from the inverse values of the slopes of the straight lines as shown in Fig. 4. The estimated temperature may have an associated error arising from uncertainty in the slope of straight lines as shown in the figure. The linear slope for hot region in the plot indicates that the primary electron distribution is Maxwellian (Holmes 1982).

As both hot and cold electrons behave as Maxwellian, we can use the following sets of equations to estimate the density of hot (N_{ch}) and cold (N_{ec}) electrons respectively (Yamazumi and Ikezawa 1990),

$$N_{ec} = 4\, I_{ec}/eA_p\,(8\, kT_{ec}/\pi m)^{1/2}, \tag{2}$$

$$N_{ch} = 4\, I_{eh}/eA_p\,(8\, kT_{eh}/\pi m)^{1/2}. \tag{3}$$

In the above expressions, I_{ec} and I_{eh} are the cold electron and hot electron saturation currents respectively, e and m are the elementary charge and the electron mass respectively, A_P is the probe surface area, T_{ec} is the

https://doi.org/10.1017/S0022377812000815 Published online by Cambridge University Press

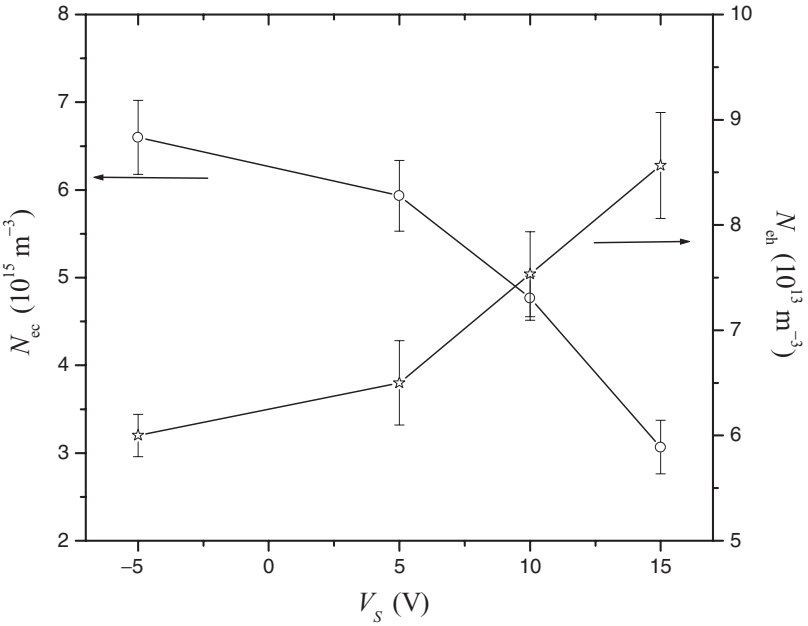


Figure 5. Variation of hot (N_{ch}) and cold (N_{ec}) electron densities with change in V_S.

temperature of cold electrons, and T_{eh} is the temperature of hot electrons.

To estimate the density of hot electrons, the current corresponding to the negative probe bias V_B, equal to the energy of hot electrons ($-V_B = T_{eh}/e$), is considered to be the hot electron current. In the semi-log plot (Fig. 4), the estimated energy of hot electrons is found to be 15 eV and 23 eV for $V_S = 5$ V and 15 V respectively. For these two sets of data, the current corresponding to the probe bias of –15 V and –23V is used to estimate the density of hot electrons.

For cold electrons, the current corresponding to a fixed probe bias of 25 V (which is above plasma potential for all applied V_S) is used to estimate the density using relation (2). Although at $V_B = 25$ V, both hot and cold electrons can contribute to the probe current, but due to low density of hot component, their contributions can be neglected.

The ratio of the hot electron current to the cold electron current I_{eh}/I_{ec} is approximately of the order of 10^{-2}.

For each cage bias V_S, the current and density values of both hot and cold electrons are estimated in a similar manner.

The density values of cold and hot electrons calculated from relations (2) and (3) for different V_S values are found to be in the range of 10^{15} m^{-3} and 10^{13} m^{-3} respectively. The values of cold and hot electron density estimated by this method are found to be in acceptable range for multi-dipole devices. The order of density of hot electrons suggests that hot electrons are nothing but primary electrons behaving like Maxwellian electrons. Earlier, Leung et al. (1976) also found that the density of plasma electrons is almost 100 times higher than the density of primary electrons in a similar device.

Variations in hot (N_{ch}) and cold (N_{ec}) electron density values for different cage bias voltage values, V_S are shown in Fig. 5. It is found that the density of cold electrons decreases with increase in positive bias applied to the cage, whereas density of hot electrons increases. From this observation, we can say that the positively biased magnetic cage almost acts as a Maxwell's demon (MacKenzie et al. 1971). The observed increase in hot (N_{ch}) electrons density may be due to increase in the number of emitted primary electrons from the filaments because of the positive plasma potential, which floats few volts above the applied V_S. Earlier, Nakamura and Nomura (1978) reported this phenomenon in a multi-dipole device. In addition, hot primary electrons may transfer energy to cold plasma electrons by collisional process, thereby increasing the loss of cold electrons from the cusp region (Knorr and Merlino 1984). Therefore, increase in positive plasma potential has a two-fold effect: It increases the number of hot primary electrons emitted from the filaments, and enhances the loss of cold plasma electrons at the cusp.

Probably for these two reasons, the ratio of the density of hot to cold electrons N ($=N_{eh}/N_{ec}$) is found to increase with increase in cage bias voltage V_S. This is also shown in Fig. 6. The value of N is approximately 10^{-2}.

Again, variations in ion (N_i) and cold electron density (N_{ec}) values with change in V_S values are shown in Fig. 7. This plot indicates the balance of charged particles in the plasma system. Due to the continuity of the current, ion current to the probe should increase when electron current to the cage increases.

Further, the ratio of the density of hot electrons (primary) to plasma ions N_{eh}/N_i is found to be 10^{-2}, which agrees with the result of Lang and Hershkowitz (1978).

Generally, when the magnetic cage is positively biased, the effective discharge voltage experienced by primary electrons increases (Cho et al. 1990). Although we have

https://doi.org/10.1017/S0022377812000815 Published online by Cambridge University Press

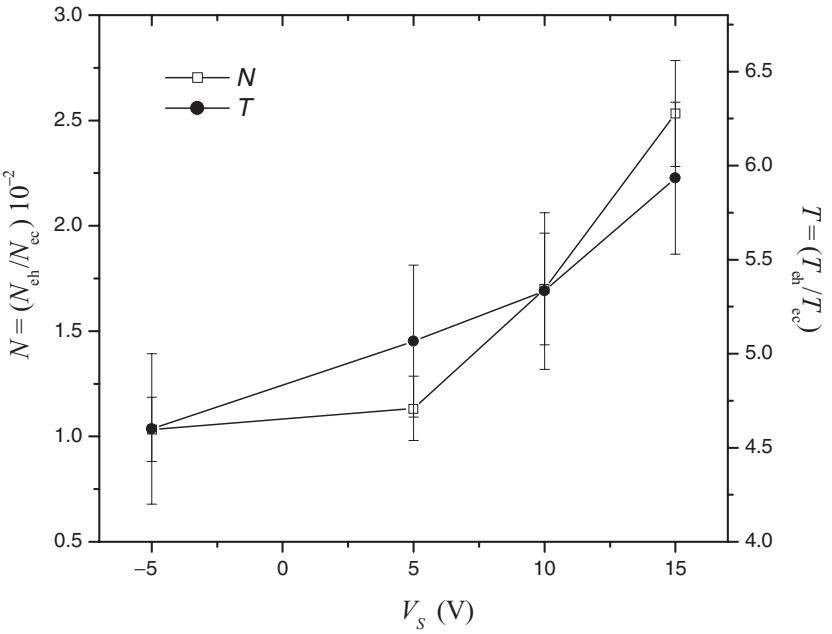


Figure 6. The ratio of hot to cold electron densities (N) and temperature (T) is plotted for different V_S values.

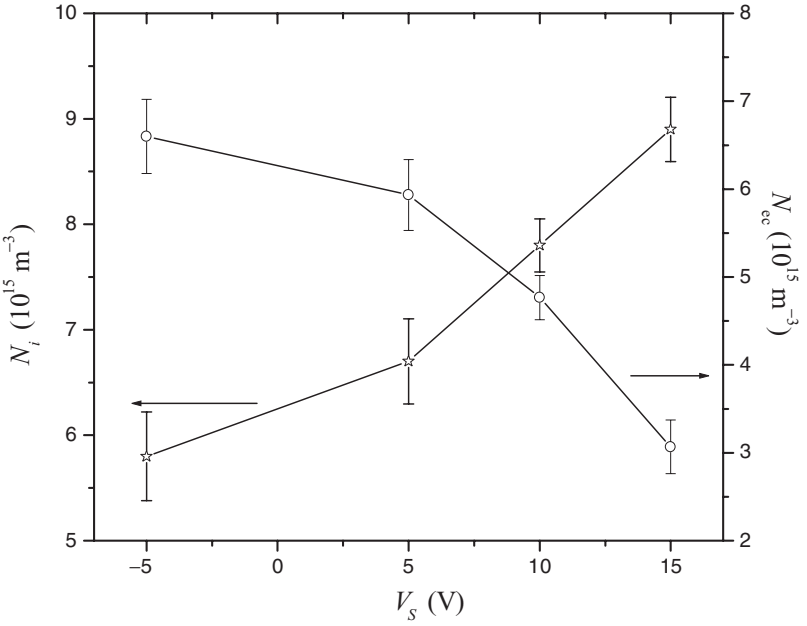


Figure 7. Variation of ion density (N_i) and cold electron density (N_{ec}) with change in V_S.

observed that the energy (temperature) of both cold and hot electrons increases, the energy of hot electrons is highly influenced by the applied cage biasing voltage V_S. The energy of hot electrons increases from 14 eV to 23 eV but energy of cold electrons increases from 3 eV to 4.2 eV when V_S is increased from –5 V to 15 V. The plasma always floats a few volts above the applied positive cage biasing voltage to prevent further loss of electrons. This enhanced plasma potential tends to accelerate the ionizing electrons (primary) as soon as they enter the plasma.

The variations of plasma potential, floating potential, cold and hot electron temperature with the cage biasing voltage V_S are given in Table 1 for a particular set of data.

The primary electrons emitted by hot filaments (cathode) possess an initial energy $E_P \approx e\,(V_P + V_D)$, where V_P is the plasma potential and V_D is the discharge voltage. The observed increase in energy of hot electrons with the positive cage bias voltage V_S (or with increasing plasma potential) may be due to the initial acceleration experienced by primary electrons.

The cold electrons are produced in pairs with ions in the ionization process. Small increase in temperature of cold electrons is also possible due to increase in energy of primary electrons. The cold electrons may get

https://doi.org/10.1017/S0022377812000815 Published online by Cambridge University Press

Table 1. Variation of plasma potential, floating potential, and cold and hot electron temperatures with the cage biasing voltage, V_S.

V_S (V)	V_P (V)	V_f (V)	$V_P - V_f$ (V)	Calculated T_e (eV)	T_{ec} (eV)	T_{eh} (eV)
−5	0	−14	14	2.69	3	14
5	6	−8.5	14.5	2.78	3.2	15
10	14	−2.3	16.3	3.13	3.6	18
15	23.5	5.7	17.8	3.42	4.2	23

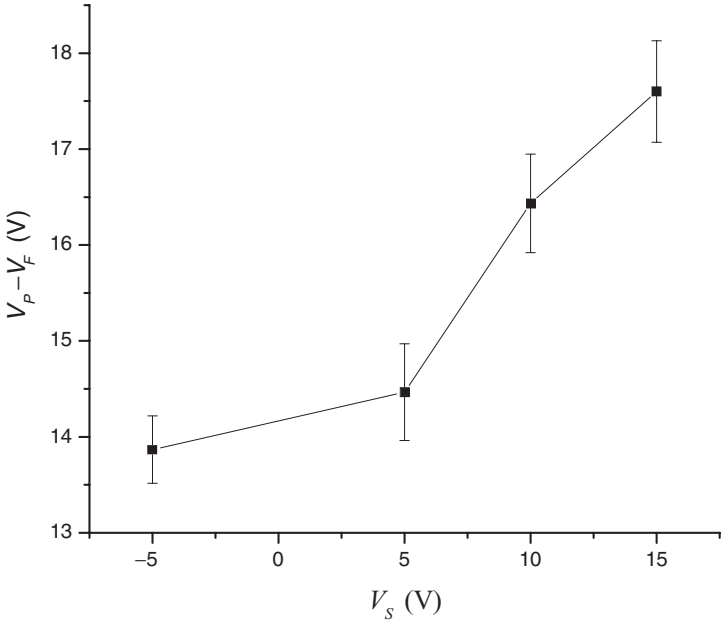


Figure 8. Difference of plasma potential and floating potential $V_P - V_f$ is plotted against V_S.

energized due to collisional energy transfer from hot primary electrons to cold plasma electrons (Knorr and Merlino 1984).

The observed increase in temperature of cold electrons can also be interpreted from increase in plasma potential caused by the applied cage biasing voltage V_S. To stop the excess bleeding of electrons to the positively biased magnetic cage, the plasma potential must be approximately equal to the electron (cold) thermal energy T_{ec} (Ganguli and Tarey 2002)

Further, it is observed that the plasma potential V_P, the floating potential V_f, and their difference $V_P - V_f$ increases with increase in cage biasing voltage V_S. The increase in difference also indicates a rise in cold electron temperature (T_{ec}).

In a multi-dipole discharge plasma like ours, where speed of the plasma electrons is considerably higher than that of positive ions, at relatively high neutral pressure (10^{-4} mbar and above), the relation between plasma potential (V_P) and floating potential (V_f) can be expressed as (Hershkowitz 1989),

$$V_P - V_f = (3.3 + 0.5 \ln \mu)\, T_{ec}/e, \tag{4}$$

where T_{ec} is the electron temperature (cold) and μ is the ion mass ratio normalized to hydrogen. For our argon plasma, (4) can be written as

$$e(V_P - V_f)/5.2 = T_{ec}(\text{In eV}). \tag{5}$$

The plasma potential V_P is obtained from the probe potential that corresponds to the peak of the first derivative of the probe characteristics, and the floating potential V_f is obtained from the probe potential that corresponds to zero probe current. The variation in $V_P - V_f$ with increase in V_S is shown in Fig. 8. Thus, according to (5), there must be a rise in cold electron temperature T_{ec}. This indicated that rise in electron temperature T_{ec} is further verified from the ln $I_e - V_B$ plot of probe characteristics shown as in Fig. 4. The energy of cold electrons is found to increase from 3 eV to 4.2 eV.

Thus, increase in effective discharge voltage (effective primary electron energy) may contribute to increase in energy (temperature) of both hot and cold electrons. The effective primary electron energy e ($V_P + V_D$) and estimated energy of hot electrons are plotted in Fig. 9 for different cage biasing voltage values, V_S.

The ratio of hot and cold electron temperatures ($T = T_{he}/T_{ec}$), obtained from the ln $I_e - V_B$ plots, is plotted against V_S in Fig. 6. This ratio is found to increase from 4.6 to 5.5 with increase in V_S.

The double derivative of probe characteristics ($d^2 I/dV^2$), which is proportional to the electron energy

https://doi.org/10.1017/S0022377812000815 Published online by Cambridge University Press

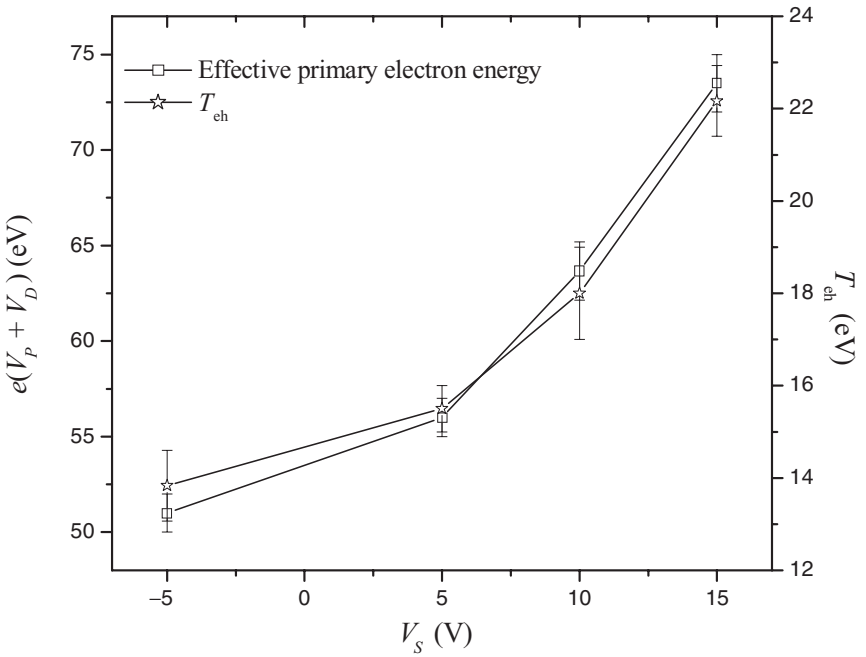


Figure 9. Variation of effective primary electron energy $e\ (V_P + V_D)$ and estimated temperature of hot electrons (T_{eh}) for different V_S values.

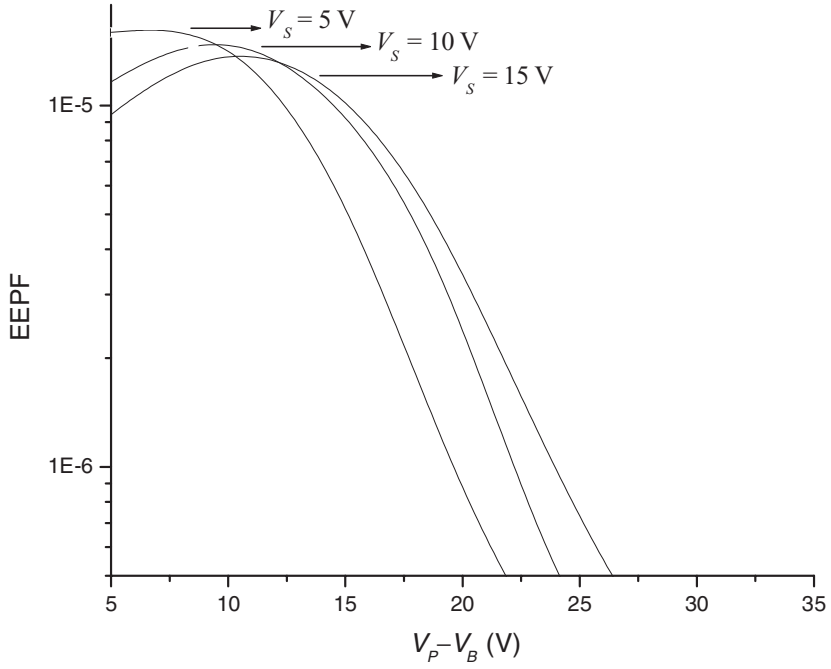


Figure 10. The bi-Maxwellian EEPFs obtained from the double derivative of probe characteristics is plotted for different V_S values.

probability functions (EEPF), is shown in Fig. 10 for different V_S values.

Along the x-axis, the difference between the plasma potential V_P and probe bias voltage V_B is plotted, which is again proportional to electron energy in the retarding field region of probe characteristics. These plots show bi-Maxwellian EEPFs, indicating the presence of two types of electrons with different temperatures (Godyak et al. 1993).

4. Conclusion

In multi-dipole discharge plasma, at pressure above 10^{-4} mbar, primary electrons (hot) exhibit Maxwellian distribution in addition to thermal plasma electrons.

The potential applied to the magnetic cage can be used to control the densities of both hot and cold electrons. Charged particle balance is observed under different biasing conditions. The bias applied to the cage mainly influences the energy of primary electrons, which

https://doi.org/10.1017/S0022377812000815 Published online by Cambridge University Press

in turn causes an increase in cold electron temperature. The cold electrons may get energized due to collisional energy transfer from the hot primary electrons to the cold plasma electrons. The method, which has been employed to estimate the densities of hot and cold electrons, provides an acceptable range for the device.

The energy of primary electrons increases because of increase in effective discharge voltage. Although the primary electrons behave as Maxwellian electrons, they retain some portion of the initial acceleration provided by the positive plasma potential. The positive plasma potential caused by the applied cage bias voltage may enhance the number of primary electrons emitted from the filaments, which in turn increases the hot electron density over the cold electron density. Further, the loss of cold plasma electrons from the cusp region increases due to collisional energy transfer from hot primary electrons.

The EEPFs obtained at different cage biasing potentials are found to be bi-Maxwellian, which indicates the presence of two types of electrons with different temperatures.

The control of hot to cold electron densities may be useful for production of negative ions in multi-dipole devices, which require very low electron temperature with higher density. In addition, the hot electrons are suitable for production of reactive species in plasma, and cold components are suitable for deposition of thin films.

The control of both cold and hot electron temperature is also essential for ion source. An increase in plasma potential and temperature will greatly enhance the loss of ions from the chamber, thereby reducing the efficiency of the source. By applying suitable bias to the cage, appropriate suitable cold electron temperature with desired density can be obtained.

References

Andreu, J., Sardin, G., Esteve, J. and Morenza, J. L. 1985 *J. Phys. D: Appl. Phys.* **18**, 1339.

Bosch, R. A. and Merlino, R. L. 1986 *Rev. Sci. Instrum.* **57**, 2940.

Chan, C., Intrator, T. and Hershkowitz, N. 1982 *Phys. Lett.* **91A**, 167.

Cho, M.-H., Hershkowitz, N. and Intrator, T. 1990 *J. Appl. Phys.* **67**, 3254.

Ganguli, A. and Tarey, R. D. 2002 *Curr. Sci.* **83**, 279.

Godyak, V. A., Piejak, R. B. and Alexandrovich, B. M. 1993 *J. Appl. Phys.* **73**, 3657.

Hershkowitz, N. 1989 *Plasma Diagnostics, Discharge Parameters and Chemistry*, Vol. 1, Boston, MA: Academic, ch. 3.

Hershkowitz, N., Cho, M.-H. and Pruski, J. 1992 *Plasma Source Sci. Technol.* **1**, 87.

Hershkowitz, N., Hendricks, K. and Carpenter, R. T. 1982 *J. Appl. Phys.* **53**, 4105.

Hershkowitz, N. and Leung, K. N. 1975 *Appl. Phys. Lett.* **26**, 607.

Holmes, A. J. T. 1982 *Rev. Sci. Instrum.* **53**, 1517.

Knorr, G. and Merlino, R. L. 1984 *Plasma Phys. Contr. Fusion* **26**, 433.

Lang, A. and Hershkowitz, N. 1978 *J. Appl. Phys.* **49**, 4707.

Leung, K. N., Hershkowitz, N. and Mackenzie, K. R. 1976 *Phys. Fluids* **19**, 1045.

Leung, K. N., Samec, T. K. and Lamm, A. 1975 *Phys. Lett.* **51A**, 490.

Limpaecher, R. and MacKenzie, K. R. 1973 *Rev. Sci. Instrum.* **44**, 726.

MacKenzie, K. R., Taylor, R. J., Cohn, D., Ault, E. and Ikezi, H. 1971 *Appl. Phys. Lett.* **18**, 529.

Merlino, R. L. 2007 *Am. J. Phys.* **75**, 1078.

Mishra, M. K., Phukan, A., Chakraborty, M. and Goswami, K. S. 2007 *Phys. Lett. A* **365**, 135.

Nakamura, Y. and Nomura, Y. 1978 *Phys. Lett.* **65A**, 415.

Oertl, M. and Skoelv, A. 1984 *Proceedings of the International Conference on Plasma Physics*, Lausanne, Switzerland, **331**.

Phukan, A., Mishra, M. K. and Chakraborty, M. 2007 *J. Phys. D. Appl. Phys.* **40**, 3616.

Pilling, L. S. and Carnegie, D. A. 2007 *Plasma Sources Sci. Technol.* **16**, 570.

Pustylnik, M., Ohno, N. and Takamura, S. 2006 *Jpn. J. Appl. Phys.* **45**, 926.

Ruscanu, D., Anita, V. and Popa, G. 2000 *Eur. Phys. J.* D **10**, 449.

Yamazumi, T. and Ikezawa, S. 1990 *Jpn. J. Appl. Phys.* **29**, 1807.

https://doi.org/10.1017/S0022377812000815 Published online by Cambridge University Press